coatings

MDPI

Article

Preparation and Anticorrosive Property of Soluble Aniline Tetramer

Yongbo Ding *, Jia Liang, Gaofeng Liu, Wenting Ni and Liang Shen *

The Department of Coatings and Polymeric Materials, Jiangxi Science and Technology Normal University, Nanchang 330013, China; Liangjia_123@126.com (J.L.); 18279155260@sina.cn (G.L.); niwenting@cosuzuka.com (W.N.)

* Correspondence: yongboding@jxstnu.com.cn (Y.D.); liangshen@jxstnu.com.cn (L.S.); Tel.: +86-0791-8381-5321 (Y.D.)

Received: 17 May 2019; Accepted: 17 June 2019; Published: 20 June 2019

Abstract: Soluble aniline tetramer (AT) was successfully prepared by chemical oxidation method. Fourier transform infrared spectroscopy (FTIR) and ultraviolet-visible spectroscopy (UV-vis) were used to characterize its structure. The redox behavior of AT was identified through the electrochemical cyclic voltammetry studies. Then, the epoxy coating was prepared by using AT as inhibitor. Its anticorrosive property was evaluated by salt solution resistance test, polarization curve, and electrochemical impedance spectroscopy (EIS). Salt solution resistance test, polarization curves, and EIS measurements indicate that the obtained epoxy anticorrosive coating, containing 1.0% AT, exhibits remarkably enhanced corrosion protection properties on Q235 steel electrodes as compared to pure epoxy anticorrosive coating without AT. The significantly improved anticorrosion performance may be owing to the redox behavior of the AT, adsorption and inhibition effect of AT on Q235 steel surface, as well as synergistic curing effect by AT and polyamide.

Keywords: aniline tetramer; solubility; electroactivity; corrosive inhibition; adsorption and inhibition effect; synergistic curing effect

1. Introduction

Just like other natural hazards (earthquakes, tornadoes, or hurricanes), corrosion can cause severe and expensive damage to everything from automobiles to infrastructure (pipelines, buildings, bridges, and military). The important method in corrosion control is incorporation of corrosion protective (inhibiting) coatings and/or inhibitors [1,2]. Organic coatings can retard corrosion through a barrier or inhibition mechanism. The barrier mechanism is achieved via a coating that effectively isolates the substrate from corrosive elements [3]. Inhibition refers to a modification of the organic coating that allows transport of the inhibiting species through the aqueous environment onto the metal substrate to retard corrosion via barrier, passivation, or sacrificial mechanisms [4].

Intrinsically conducting polymers (ICPs) have been used to protect metals and their alloys [5] because of their unique characteristics, which undergo oxidation–reduction reactions. DeBerry was the pioneer that introduced polyaniline (PANI) coatings for stainless steels [6]. However, poor process ability, solubility, and dispersity of PANI limit the widespread use of PANI.

Oligoanilines analogues, such as trianiline and pentaniline, show electrochemical properties similar to those of PANI. In the meantime, the solubility of oligoanilines is much higher than that of PANI [7]. A number of anticorrosive coatings, including oligoanilines, have been developed [8–11]. However, application-oriented investigations, such as salt solution resistance tests of organic coatings with aniline oligomer as inhibitor, have seldom been developed.

Therefore, in this paper, epoxy anticorrosive coatings containing aniline tetramer (AT) as a corrosion inhibitor, were successfully prepared. Electroactivity of AT was studied through cyclic voltammetry (CV). Corrosion protection of epoxy anticorrosive coatings with different content AT (wt %) was accomplished by applying the corrosion measure technique using electrochemical principle and salt solution resistance test on Q235 steel in 3.5% NaCl solution.

2. Materials and Methods

2.1. Materials

N-Phenyl-1,4-phenylenediamine (ADPA) was purchased from Shanghai Aladdin Biochemical Technology Co., Ltd. (Shanghai, China). Ammonia, acetone, hydrochloric acid (HCl), petroleum ether, dimethyl sulfoxide (DMSO), tetrahydrofuran (THF), anhydrous ethanol (EtOH), ammonium persulfate (APS), toluene, and N,N-Dimethylformamide (DMF) were purchased from Tianjin Fuchen chemical reagent Co., Ltd. (Tianjin, China). The above-mentioned chemicals were of analytical grade and used without further purification. Technical-grade epoxy Resin 6101 and polyamide resin 650 were purchased from Hong Kong Rongfa decoration materials Co., Ltd. (Dongguan, China). Technical-grade BYK-110 and BYK-306 were both supplied by BYK Additives and Instruments. The specifications and pretreatment of the Q235 steel specimens and Q235 steel electrodes are the same as those in reference [12].

2.2. Preparation of Aniline Tetramer

The preparation of aniline tetramer was based on the method reported in Sun Zaicheng's literature [13]. According to Sun Zaicheng's literature [13], the main product is aniline tetramer. The specific steps were as follows: N-Phenyl-1,4-phenylenediamine (ADPA) (1.84 g) was dissolved in acetone, deionized water (100 mL), and concentrated hydrochloric acid (25 mL) with vigorous stirring at 0 °C. At the same time, the ammonium persulfate (APS) (4.5 g) was dissolved in water (25 mL). The APS solution was added to the stirred mixture drop by drop. The reaction took 3 h at 0 °C; then, the product was precipitated through a large amount of petroleum ether. Following this, the precipitate was filtered and purified with a large amount of THF. Finally, the product was dried in a vacuum of 60 °C. The synthetic reaction equations and photographs of aniline tetramer are shown in Figure 1.

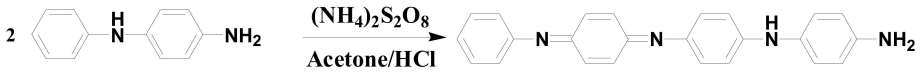

(a) Synthesis of aniline tetramer

(b) Photograph of aniline tetramer

Figure 1. Synthesis (**a**) and photograph (**b**) of aniline tetramer.

2.3. Preparation of Epoxy Anticorrosive Coating

Table 1 lists the formulations of epoxy anticorrosive coatings with different content of AT.

Table 1. Formulation of the epoxy coating with aniline tetramer as corrosion inhibitor.

wt % AT	0.0% AT	0.1% AT	0.5% AT	1.0% AT
epoxy resin(6101)	50	50	50	50
polyamide resin(650)	40	40	40	40
AT	0	0.1	0.5	1.0
DMSO	9.8	9.7	9.3	8.8
BYK-110	0.1	0.1	0.1	0.1
BYK-306	0.1	0.1	0.1	0.1
Paint thinner [1]	2–5 mL	2–5 mL	2–5 mL	2–5 mL

[1] The mixed paint thinner is butanone, cyclohexanone, butanol, and xylene by mass ratio 1:2:2:5

2.4. Characterizations

The structure of AT has high purity and was identified through FTIR (NICOLET 6700, Thermo) (Waltham, MA, USA) and UV-vis spectra (T9, PERSEE). For FTIR, AT was analyzed using the KBr pellet method, and the background spectrum was obtained from a pure KBr pellet of the same size. Scanning electron microscopy (SEM) measurements were made with a cold field emission scanning electron microscope JSM-6701F (Tokyo, Japan). The particle size and distribution of AT were characterized by use of particle size analyzer (Nicomp 380, PSS) (San Barbara, FL, USA). Dynamic thermomechanical analysis (DMA) of epoxy anticorrosive coatings were carried out based on a DuPont TA Q800 analyzer (New Castle, DE, USA) according to the method in reference [8].

The mechanical behaviors of as-prepared epoxy anticorrosive coatings under uni-axial tension (1 N/min) were measured on a dynamic thermomechanical analysis (DMA), which were performed from 30 to 150 °C with a DuPont TA Q800 analyzer at a heating rate of 3 °C /min and at a frequency of 1 Hz.

The redox behavior of AT was investigated by electrochemical cyclic voltammetric (CV) analysis. The electrochemical cyclic voltammetric was tested in 1.0 M HCl aqueous solution through a conventional three-electrode cell; working electrode: Aniline tetramer modified glassy carbon electrode (the glassy carbon electrode was immersed in a DMSO solution containing 0.2 mg/mL of AT for 2 h), reference electrode: Ag/AgCl (standard KCl) electrode, counter electrode: Pt wire.

Potentiodynamic polarization and electrochemical impedance spectroscopy (EIS) of epoxy coating with or without 1.0% AT-coated (c) Q235 steel electrodes after immersion in 3.5% NaCl for 24 h were performed using a CHI-660E workstation (Chenhua, Shanghai) according to a conventional three-electrode cell. The measurement parameters of potentiodynamic polarization and EIS were the same as those set out in reference [14].

The corrosion current density of three kinds of Q235 steel electrodes (bare and coated with epoxy coatings) in 3.5 wt.% NaCl solution were obtained through the Tafel extrapolation. To quantitatively evaluate the anticorrosive performance of Q235 steel electrode coated with epoxy coating and epoxy coating containing 1.0% AT, the EIS data were fitted by ZsimpWin3.21 software with equivalent circuits.

3. Results and Discussion

3.1. The Structure of Aniline Tetramer

FTIR spectrum of aniline tetramer is illustrated in Figure 2. We can see from Figure 2, the characteristic absorption bands at 3441cm^{-1} were ascribed to terminal –NH_2 of aniline tetramer, and the absorption bands appearing at 3399, 3356, and 3304 cm^{-1} arose from the B–NH–B (B on behalf of

the benzene ring). The absorption peaks at 3195 cm^{-1} were connected to quinone ring of HN = Q (Q on behalf of the quinone ring). The characteristic absorption peaks of benzene ring were mainly at 1592, 1497, and 1167 cm^{-1}. Further, 1304 cm^{-1} belonging to the C–N stretching vibration absorption peak, with the characteristic peak of the 1,4 substituted benzene ring, appearing at 819, 748, and 695 cm^{-1}, are characteristic peaks of disubstituted benzene rings [14].

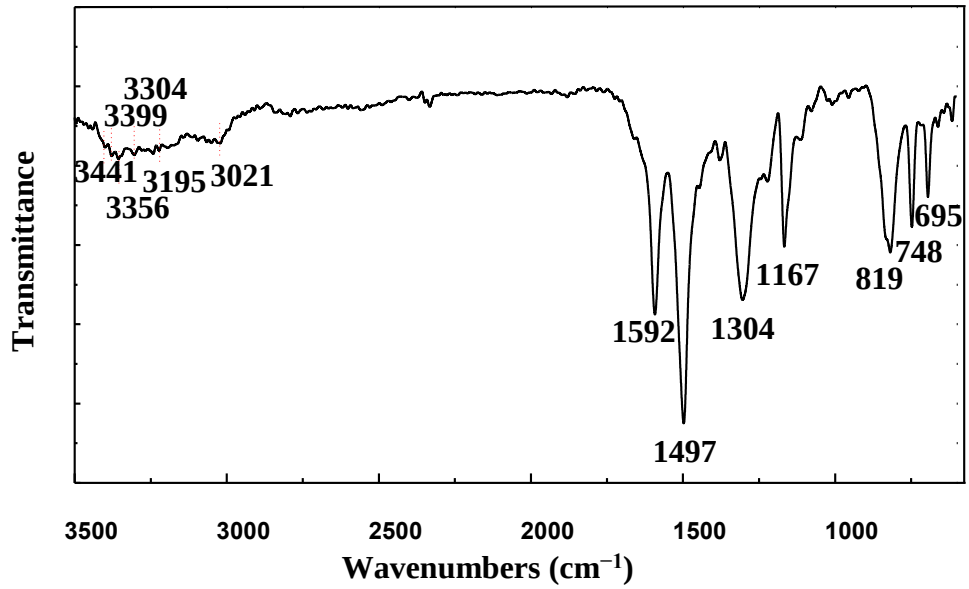

Figure 2. FTIR spectra of aniline tetramer.

Ultraviolet-visible spectroscopy (UV-vis) of aniline tetramer in DMSO is shown in Figure 3. As can be seen from Figure 3, AT demonstrated two apparent absorption peaks at 322 and 576 nm (curve in Figure 3), which were ascribed to the $\pi \rightarrow \pi^*$ transition of the benzene ring and the benzenoid (B) to quinoid (Q) $\pi_B \rightarrow \pi_Q$ excitonic transition. Thus, the structure of as-prepared aniline tetramer showed no difference compared to the previous reference report [15].

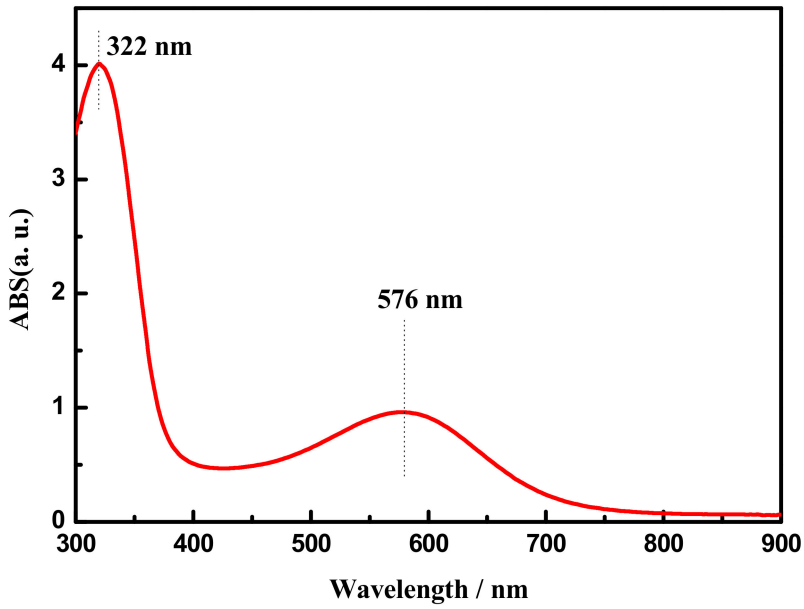

Figure 3. UV-vis spectra of aniline tetramer measured in dimethyl sulfoxide (DMSO).

3.2. The Solubility of Aniline Tetramer

The solubility of as-prepared aniline tetramer in different solvents was studied according to reference [16]. From Figure 4, we can obviously see AT exhibited solubility in common organic solvents at room temperature. In addition, the solubility of AT in common organic solvents was also summarized in Table 2.

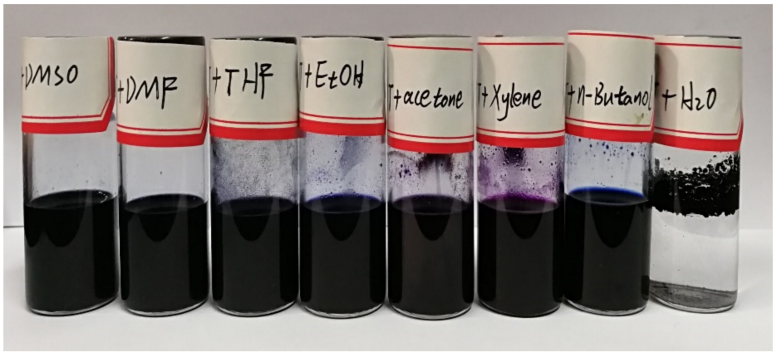

Figure 4. Solubility experiments of aniline tetramer in different solvents.

Table 2. Solubility of aniline tetramer (AT) in commonsolvents.

Solvents	DMSO	DMF	THF	EtOH	Acetone	Xylene	Butanol	H_2O
Solubility (mg/mL)	76.0	53.2	21.0	8.5	24.5	7.5	4.8	0.5

It should be noted that AT exhibited quite good solubility in DMSO and DMF, which might be attributable to solubility parameter of AT in between 24.8 (solubility parameter of DMF) and 26.4 (solubility parameter of DMSO). Although the solubility parameter of ethanol is 26.0, hydrogen bonding index reached 20.1 due to its strong hydrogen bonding force [17], therefore, there is no advantage for the dissolution of the aniline tetramer. In addition, the aniline tetramer does not contain water-soluble polar groups, therefore, the solubility of aniline tetramer in water is very small, only 0.5 mg/mL.

3.3. Micromorphology and Particle Size Distribution of Aniline Tetramer

Figure 5 shows the morphology of aniline tetramers under different magnifications of scanning electron microscopy. It can be seen from the figure that the aniline tetramer particles have a particle size of about 150 nm and the particles are both fine and dense. Due to the fact that electrochemical properties of conductive polymer materials are inseparable from the particle size morphology, and packing tightness, we speculate that nanoscale aniline tetramers will be easier to disperse in the coating to produce a denser coating.

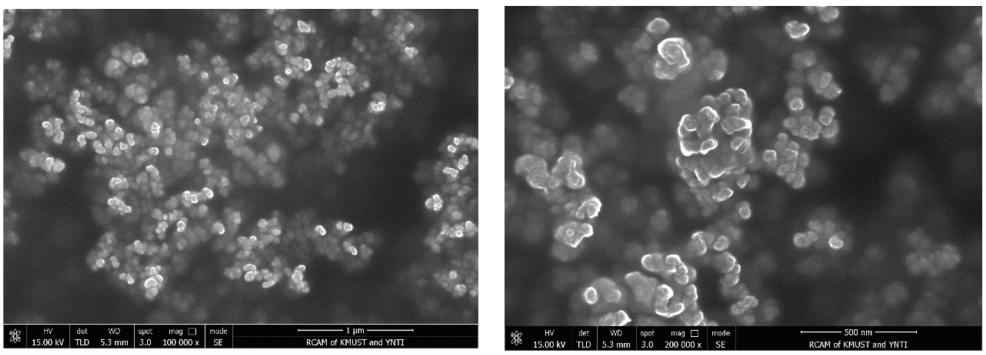

(a) (b)

Figure 5. SEM photos of aniline tetramer under different magnification: (**a**) scale bar: 1000 nm; (**b**) scale bar: 500 nm.

3.4. Redox Behavior of Aniline Tetramer

Cyclic voltammetry measurement of aniline tetramer was carried out in 1.0 M HCl solution at a scan rate of 50 mV/s, as shown in Figure 6. There were two oxidation peaks, 0.28 and 0.59 V, respectively; this is similar to an aniline trimer undergoing two steps of single electron transmission process [8]. It has been reported that polyaniline imparts excellent redox properties due to the presence of a conjugated structure in the molecular chain, and at the same time, the aniline tetramer easily forms the coordination bond with the empty d orbital of the metal due to the unshared electron pair on the central atom N, thereby forming an adsorption layer on the metal surface to inhibit corrosion [18], so we predict that the aniline tetramer with redox and adsorption will also have excellent corrosion inhibition properties.

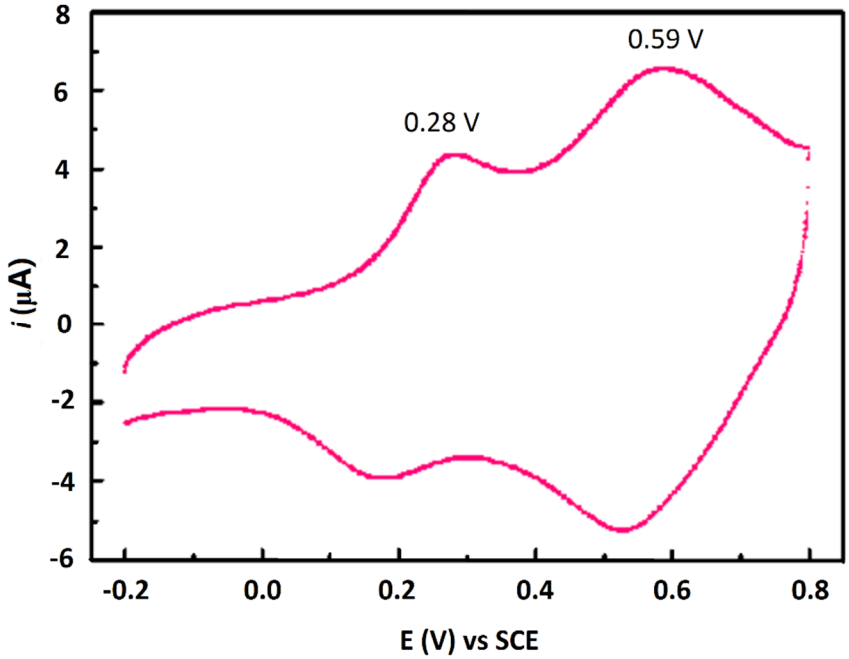

Figure 6. Cyclic voltammogram of AT in 1 M HCl solution (aniline tetramer modified glass carbon electrode used as work electrode).

3.5. Saltwater-Resistant Test of Epoxy Coatings Containing Different Content of AT

Saltwater-resistant test weighs the ability of anticorrosion coatings to withstand a combination of both salt spray and humid conditions. The epoxy coatings containing AT are expected to improve corrosion resistance. The ability to prevent corrosion is best measured through estimating the spreading of corrosion from the x-scratch made on the painted mild steel substrate [19].

The spreading of corrosion from the scribe was less in the case of panels coated with epoxy coatings containing 1.0% AT than those coated with pure epoxy coatings after 30 days of the saltwater-resistant test (Figure 7). During the saltwater-resistant test, the upper half of Q235 steel specimens were exposed to air, while the lower half of Q235 steel specimens were immersed in 3.5% NaCl solution; therefore, chloride ions attack the iron metal, forming iron (II) chloride, followed by hydrolysis and rust formation at the anodic areas (exposed bare steel in the scribed region). However, formation of passive metal oxide layers or adsorption of AT on Q235 steel surface would prevent further corrosion when epoxy coatings containing 1.0% AT [8]. Therefore, the corrosion resistance of epoxy anticorrosive coatings containing AT got better and better with the increase of AT.

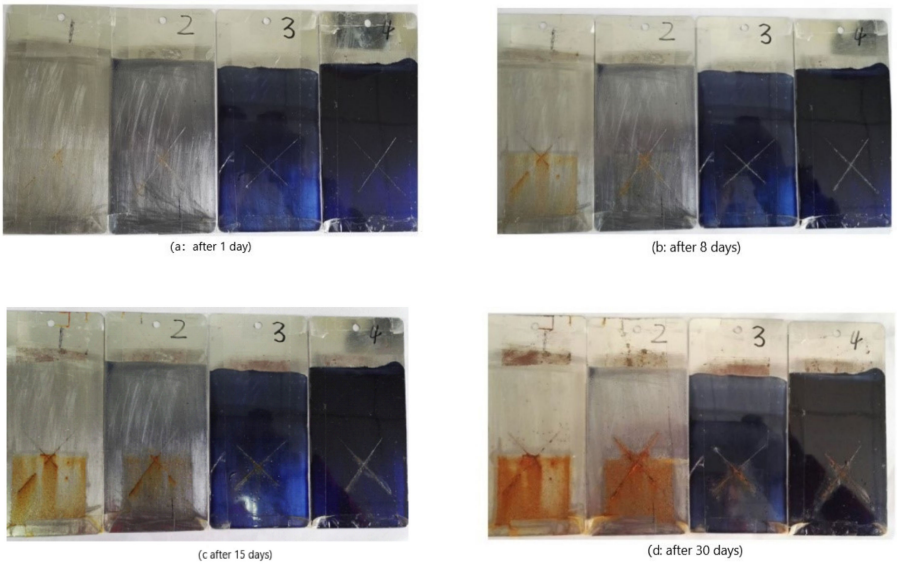

Figure 7. Corrosion behavior of epoxy coatings containing different content of AT after 3.5% NaCl solution immersion for different times(1: 0.0% AT, 2: 0.1% AT, 3: 0.5% AT, 4: 1.0% AT).

3.6. Potentiodynamic Measurements

Electrochemical measurements, such as polarization curves and EIS, are commonly applied to assess the corrosion resistance of organic coatings. Figure 8 shows polarization curves of three kinds of work electrode. As shown in Figure 8, the addition of AT increased the corrosion potential of the Q235 steel electrode from −0.59V coated with epoxy coating to −0.57V coated with epoxy coating containing 1.0% AT, demonstrating that the addition of AT effectively inhibited corrosion tendency of Q235 steel electrode [20]. At the same time, the corrosion current density could be determined by the Tafel extrapolation method. The self-corrosion current density of Q235 steel electrode coated with epoxy coating and epoxy coating containing 1.0% AT were 6.27×10^{-7} A/cm^2 and 1.26×10^{-7} A/cm^2, respectively; the self-corrosion current density of the pure Q235 steel electrode was 5.13×10^{-6} A/cm^2. The protection efficiency was 87.8% and 97.5% [15], which shows that the addition of AT can effectively inhibit the corrosion of Q235 steel electrode in 3.5% NaCl solution. The significantly improved anticorrosion performance may be attributed to the redox catalytic capabilities of the AT, adsorption and inhibition effect of AT on Q235 steel surface, as well as synergistic curing effect by AT and polyamide.

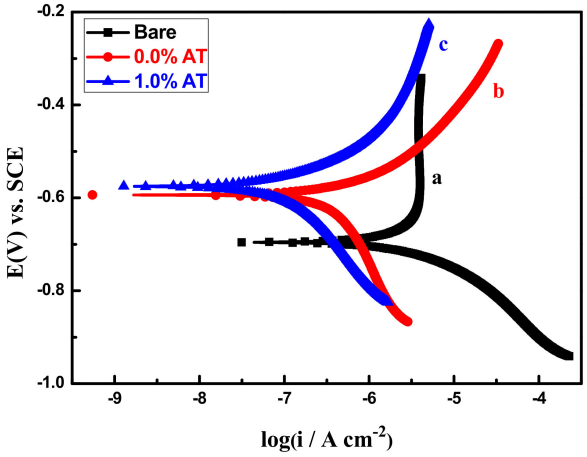

Figure 8. The polarization curves of bare (**a**), pure epoxy-coated (**b**), and epoxy coating with 1.0%AT-coated (**c**) Q235 steel electrodes after immersion in 3.5% NaCl for 24 h.

3.7. Electrochemical Impedance Measurements

Figure 9a,b shows the Nyquist and bode plots of epoxy coating with 0.0% and 1.0% AT immersed in 3.5% NaCl solution after 24 h. As can be seen from the nyquist diagram, the electrodes coated with both coatings had a capacitive reactance arc at low frequencies and a larger capacitive reactance arc at medium and high frequencies, while the two capacitive reactance arc diameters of the Q235 steel electrode coated with epoxy coating with 1.0% AT were also significantly higher than those coated with coated with epoxy coating with 0.0% AT. In addition, as seen from the bode plots, the mode resistance of Q235 steel electrode coated with epoxy coating with 1.0% AT was 25.3 kΩ at low frequencies such as 0.01 Hz, which is significantly higher than 18.1 kΩ for those coated with epoxy coating with 0.0% AT. The mode resistance corresponding to 0.01 Hz at low frequencies directly represents the ability of the coating to suppress the flow of anode and cathode currents; thus, the value of the mode resistance is directly inversely proportional to the corrosion rate of metals [21]. Therefore, the corrosion rate of the Q235 steel electrode coated with epoxy coating containing 1.0% AT is lower than that of the Q235 steel electrode coated with epoxy coating with 0.0% AT. Not only that, as can be seen from the bode phase angle diagram, the characteristic frequency at an angle of 45° of the Q235 steel electrode coated with epoxy coating containing 1.0% AT was lower than that of Q235 steel electrode coated with epoxy coating with 0.0% AT; because the characteristic frequency of the high-frequency phase angle −45° was approximately proportional to the porosity of the coating [22], the porosity of epoxy coating containing 1.0% AT was lower than that of epoxy coating containing 0.0% AT.

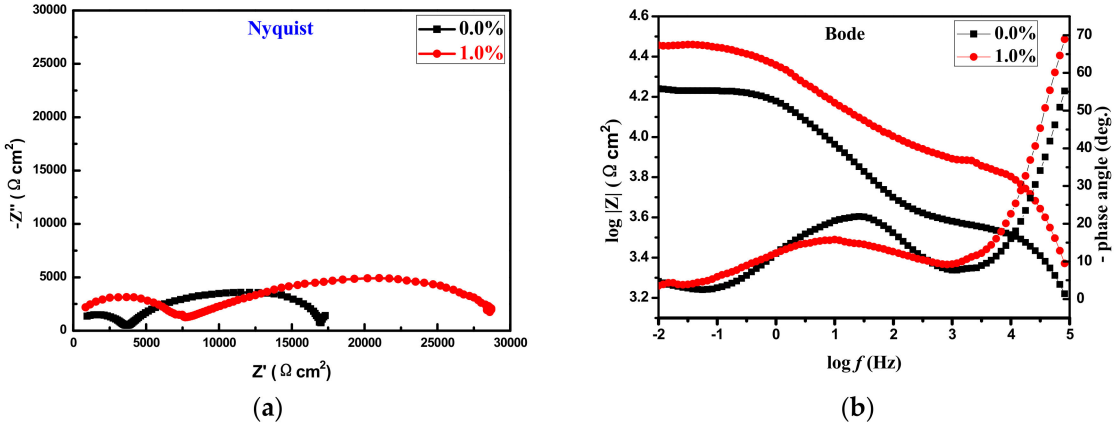

Figure 9. The Nyquist (**a**) and bode plots (**b**) of epoxy coating with 0.0% and 1.0% AT immersed in 3.5% NaCl solution after 24 h. (a) The Nyquist diagrams of epoxy coating with 0.0% and 1.0% AT immersed in 3.5% NaCl solution after 24 h; (b) The bode plots of epoxy coating with 0.0% and 1.0% AT immersed in 3.5% NaCl solution after 24 h.

For quantitatively estimating the anticorrosion properties of epoxy coating with AT, EIS data were fitted with equivalent circuit, as shown in Figure 10, and the fitted parameters are listed in Table 3. In Figure 10, R_s is the solution resistance and constant phase angle element Q is used instead of pure capacitance, because a dispersion effect may be caused between the metal/coating system [23,24]. The high-frequency elements Q_c, R_c are equal to the capacitance and coating resistance of coating; the medium-low frequency elements Q_{dl}, R_{ct} are double-layer capacitance and charge-transfer resistance, respectively [25].

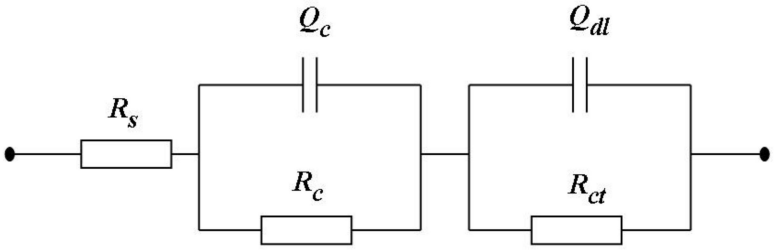

(**a**) The equivalent circuit used to fit the EIS data.

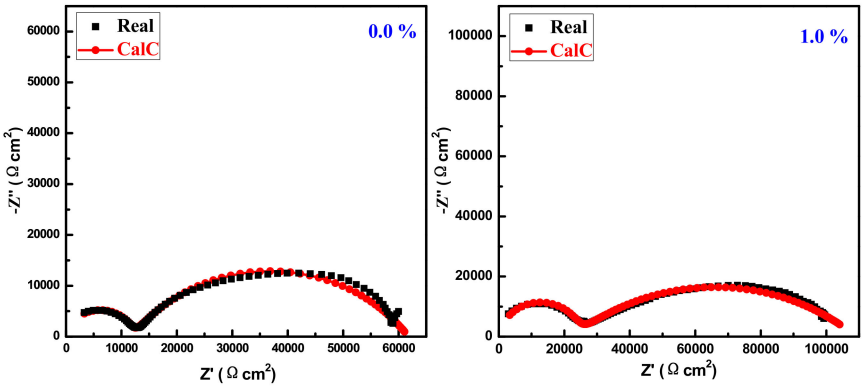

(**b**) The fitted Nyquist data from the equivalent circuit R(QR)(QR with or without AT

Figure 10. The equivalent circuit (R(QR)(QR)) (**a**) used to fit the EIS data and the fitted Nyquist data (**b**) from the equivalent circuit with or without AT.

Table 3. Fitting parameters for the electrical equivalent circuit R(QR)(QR).

Parameters	0.0% AT	1.0% AT
R_s (Ω)	0.01	0.01
Q_c (μF·cm^{-2}·Hz$^{1-n}{}_1$)	2.40	3.33
n_1	0.61	0.46
R_c (kΩ)	49.80	86.04
Q_{dl} (nF·cm^{-2}·Hz^{1-n2})	1.21	0.49
n_2	0.89	0.95
R_{ct} (kΩ)	11.98	23.08

As shown in Table 2, R_s remained equal during the two Q235 steel electrodes coated with epoxy coating. R_c represents the physical barrier properties of the coating while the R_{ct} is determined by the Faradaic process of charge transfer process. It is rather remarkable that both the R_c and R_{ct} of the Q235 steel electrode coated with epoxy coating containing 1.0% AT were found to be much higher than those of the Q235 steel electrode coated with pure epoxy coatings (86.04 vs. 49.8023.08 vs. 11.98).

In a word, both the polarization curves and EIS results clearly demonstrated that epoxy coating with 1.0% AT protect the Q235 steel against corrosion better than the pure epoxy coating does.

3.8. Mechanism of Corrosion Inhibition

It is generally known that the inhibition action of organic inhibitor originated from the adsorption of the inhibitor molecules onto the metal/solution interface [4]. For the sake of verifying the absorption and corrosion inhibition of aniline tetramers, the Q235 steel electrodes were immersed in a DMSO solution containing different concentrations of AT for 2 h, then the EIS of the Q235 steel electrodes were

tested in 3.5% NaCl solution and fitted by R(QR) equivalent circuit to the charge-transfer resistance and substituted with the formula $\theta = \frac{R_{ct}-R_{ct}^0}{R_{ct}}$ (R_{ct}^0 and R_{ct} are the charge transfer resistances without or with the corrosion inhibitor, and θ is the coverage of electrode). Table 4 lists the adsorption parameters of the aniline tetramer on the surface of the steel electrode. According to Table 4, the charge-transfer resistance increased with the increase of AT concentration, and the coverage of electrode also increased gradually, indicating that the protection efficiency was gradually enhanced. Therefore, the corrosion inhibition of AT may be ascribed to the presence of electron-rich N and aromatic rings.

Table 4. Adsorption parameter of AT on Q235 steel electrodes.

ρ(AT)/ (mg/mL)	C(AT)/ (mol/L)	R_{ct} ($\Omega \cdot cm^2$)	θ	$1/\theta$	$1/(10^4$ C)
Blank	–	92.2	–	–	–
0.025	6.87×10^{-5}	110.0	0.16	6.25	1.46
0.05	1.37×10^{-4}	129.3	0.29	3.45	0.73
0.10	2.75×10^{-4}	160.0	0.42	2.38	0.36
0.20	5.50×10^{-4}	181.3	0.49	2.04	0.18

Nevertheless, the amino and imino groups of aniline tetramer can also crosslink and cure with the epoxy resin and produce the shielding effect [26]. Therefore, epoxy coating with or without AT was characterized by dynamic thermomechanical analysis.

As shown in Figure 11, the epoxy coating without AT had only one peak, and the glass transition temperature (Tg) was 316.9 K. While there were two peaks in the epoxy coating with 1.0 AT, and the peak at 304.2 K corresponded to the Tg of the epoxy 6101 resin and the polyamide 650 resin curing reaction, another peak at 333.4 K corresponded to the Tg of the epoxy 6101 resin, polyamide 650 resin, and aniline tetramer synergistic curing reaction, which was higher than 316.9 K because the aniline tetramer also synergistically cured epoxy 6101 resin, causing the epoxy coating to have a larger cross-linking density, ultimately beneficial to the shielding of air and moisture. Therefore, the corrosion inhibition of AT may also be attributed to the synergistic curing reaction of aniline tetramer.

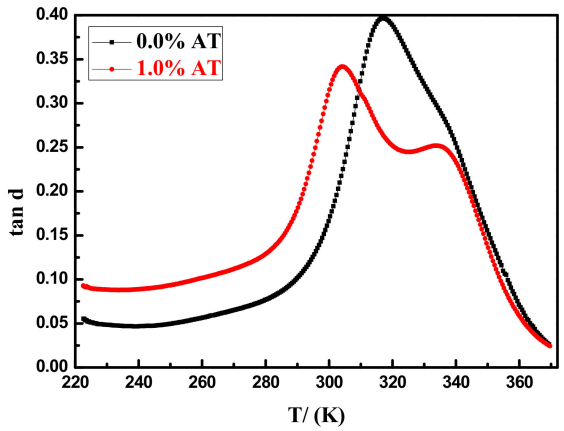

Figure 11. The dynamic thermomechanical analysis (DMA) curves of epoxy coating with 0.0% and 1.0% AT.

Therefore, it can be seen from the redox property and adsorption mechanism of aniline tetramer that the inhibition effect of aniline tetramer on Q235 not only includes the passivation of aniline tetramer on the iron surface, but also the corrosion inhibition effect of adsorption and shielding corrosion inhibition of epoxy resin after cross-linking and solidification.

4. Conclusions

(1) The aniline tetramer was successfully prepared by chemical oxidation, and the results showed that the solubility of aniline tetramer in dimethyl sulfoxide was up to 76.0 mg/mL and AT powder with an average grain size less than 150 nm and an even grain distribution.

(2) The corrosion inhibitor of epoxy coating increased gradually with the increase of the content of aniline tetramer in epoxy anticorrosive coating from 0% to 1.0%; no blister was found on the surface of the coating after 720 h 3.5% NaCl solution immersion test.

(3) By analyzing the polarization curves and EIS, it is known that the epoxy coating with 1.0% AT is significantly better than the bare epoxy coatings, Additionally, when the aniline tetramer content was 1.0%, its inhibition efficiency was up to 97.5%. Through the analysis of anti-corrosion mechanism of AT on Q235 steel, there are passivation corrosion inhibition, adsorption inhibition, and shielding corrosion inhibition.

Author Contributions: Formal analysis, G.L.; Investigation, Y.D., J.L. and W.N.; Project Administration, Y.D.; Supervision, L.S.; Writing—Review and Editing, Y.D.

Funding: The research is financially supported by the National Natural Science Foundation of China (No. 51563011) and scientific research foundation of Jiangxi Science and Technology Normal University (No. 3000990309).

Conflicts of Interest: The author declares no conflict of interest.

References

1. Szubert, K.; Wojciechowski, J.; Karasiewicz, J.; Maciejewski, H.; Lota, G. Corrosion-protective coatings based on fluorocarbosilane. *Prog. Org. Coat.* **2018**, *123*, 374–383. [CrossRef]
2. Bahrani, A.; Naderi, R.; Mahdavian, M. Chemical modification of talc with corrosion inhibitors to enhance the corrosion protective properties of epoxy-ester coating. *Prog. Org. Coat.* **2018**, *120*, 110–122. [CrossRef]
3. TabkhPaz, M.; Park, D.Y.; Lee, P.C.; Hugo, R.; Park, S.S. Development of nanocomposite coatings with improved mechanical, thermal, and corrosion protection properties. *J. Compos. Mater.* **2018**, *52*, 1045–1060. [CrossRef]
4. Ahamad, I.; Prasad, R.; Quraishi, M.A. Adsorption and inhibitive properties of some new Mannich bases of Isatin derivatives on corrosion of mild steel in acidic media. *Corros. Sci.* **2010**, *52*, 1472–1481. [CrossRef]
5. Deshpande, P.P.; Jadhav, N.G.; Gelling, V.J.; Sazou, D. Conducting polymers for corrosion protection: A review. *J. Coat. Technol. Res.* **2014**, *11*, 473–494. [CrossRef]
6. Deberry, D.W. Modification of the electrochemical and corrosion behavior of stainless steels with an electroactive coating. *J. Electrochem. Soc.* **1985**, *132*, 1022–1026. [CrossRef]
7. Ji, W.F.; Chu, C.M.; Hsu, S.; Lu, Y.D.; Lu, Y.C.; Santiago, K.S.; Yeh, J.M. Synthesis and characterization of organo-soluble aniline oligomer-based electroactive doped with gold nanoparticles, and application to electrochemical sensing of ascorbic acid. *Polymer* **2017**, *128*, 218–228. [CrossRef]
8. Huang, K.Y.; Shiu, C.L.; Wu, P.S.; Wei, Y.; Yeh, J.M.; Li, W.T. Effect of amino-capped aniline trimer on corrosion protection and physical properties for electroactive epoxy thermosets. *Electrochim. Acta* **2009**, *54*, 5400–5407. [CrossRef]
9. Chang, K.C.; Huang, K.Y.; Hsu, C.H.; Ji, W.F.; Lai, M.C.; Huang, W.; Chuang, T.L.; Yeh, J.M. Synthesis of ultra-high-strength electroactive polyimide membranes containing oligoaniline in the main chain by thermal imidization reaction. *Eur. Polym. J.* **2014**, *56*, 26–32. [CrossRef]
10. Peng, C.W.; Hsu, C.H.; Lin, K.H.; Li, P.L.; Hsieh, M.F.; Wei, Y.; Yeh, J.M.; Yu, Y.H. Electrochemical corrosion protection studies of aniline-capped aniline trimer-based electroactive polyurethane coatings. *Electrochim. Acta* **2011**, *58*, 614–620. [CrossRef]
11. Lin, S.C.; Wu, C.S.; Yeh, J.M.; Liu, Y.L. Reaction mechanism and synergistic anticorrosion property of reactive blends of maleimide-containing benzoxazine and amine-capped aniline trimer. *Polym. Chem.* **2014**, *5*, 4235–4244. [CrossRef]
12. Ye, Y.; Zhang, D.; Liu, Z.; Liu, W.; Zhao, H.; Wang, L.P.; Li, X.G. Anti-corrosion properties of oligoaniline modified silica hybrid coatings for low-carbon steel. *Synth. Met.* **2018**, *235*, 61–70. [CrossRef]

13. Sun, Z.C.; Kuang, L.; Jing, X.B.; Wang, X.L.; Li, J.L.; Wang, F.S. Synthesis of phenyl/amino-capped Tetraaniline by Chemical and Electrochemical Methods. *Chem. J. Chin. Univ.* **2002**, *23*, 496–499. [CrossRef]
14. Sun, Z.C.; Li, J.; Wang, X.H.; Wang, F.S. Synthesis and characterization of oligoanilines. *Chin. Polym. Bull.* **2001**, *1*, 16–24. [CrossRef]
15. Gu, L.; Liu, S.; Zhao, H.; Yu, H.B. Anticorrosive oligoaniline-contained electroactive siliceous hybrid materials. *RSC Adv.* **2015**, *5*, 56011–56019. [CrossRef]
16. Ding, Y.B.; Liu, Y.F.; Liu, Y.Q.; Shen, L. Preparation and anticorrosive property of carboxylated aniline trimer. *Paint Coat. Ind.* **2017**, *47*, 14–19.
17. Wu, L.M.; Li, D.; You, B. *Formulation Design of Modern Coatings*, 1st ed.; Chemical Industry Press: Beijing, China, 2001; pp. 69–70.
18. Quraishi, M.A. Electrochemical and theoretical investigation of triazole derivatives on corrosion inhibition behavior of copper in hydrochloric acid medium. *Corros. Sci.* **2013**, *70*, 161–169. [CrossRef]
19. Jegannathan, S.; Narayanan, T.S.N.S.; Ravichandran, K. Evaluation of the corrosion resistance of phosphate coatings obtained by anodic electrochemical treatment. *Prog. Org. Coat.* **2006**, *57*, 392–399. [CrossRef]
20. Shao, H.B.; Wang, X.Y.; Wang, J.M.; Wang, J.B.; Zhang, J.Q.; Cao, C.N. The cooperative inhibition effects of alkaline earth metal ions and EDTA on the corrosion of pure aluminum in an alkaline solution. *Acta Phys-Chim. Sin.* **2006**, *22*, 312–315. [CrossRef]
21. Zhao, Y.; Gao, M.; Jiming, H.U.; Cao, C. Electrochemical Investigation of Corrosion Performance of Electrophoretic Hybrid Epoxy-silane Coatings on Galvanized Steel. *Corros. Sci. Prot. Technol.* **2016**, *28*, 407–414. [CrossRef]
22. Liu, L.; Hu, J.M.; Zhang, J.Q.; Cao, C. Evaluation of protectiveness of organic coatings by means of high-frequency EIS measurement. *Corros. Sci. Prot. Technol.* **2010**, *22*, 325–328. [CrossRef]
23. Sun, H.; Liu, S.; Sun, L. A Comparative study on the corrosion of galvanized steel under simulated rust layer solution with and without 3.5wt%NaCl. *Int. J. Electrochem. Sci.* **2013**, *8*, 3494–3509. [CrossRef]
24. Liu, S.; Sun, H.; Sun, L.; Fan, H.J. Effects of pH and Cl^-, concentration on corrosion behavior of the galvanized steel in simulated rust layer solution. *Corros. Sci.* **2012**, *65*, 520–527. [CrossRef]
25. Gu, L.; Liu, S.; Zhao, H.; Yu, H.B. Facile Preparation of water-dispersible graphene sheets stabilized by carboxylated oligoanilines and their anticorrosion coatings. *ACS Appl. Mater. Interfaces* **2015**, *7*, 17641–17648. [CrossRef]
26. Chen, Y.D.; Zeng, Z.X.; Peng, S.S.; Zhang, Z.P. Preparation and properties of epoxy resin anticorrosive coating cured by aniline trimer. *Surf. Technol.* **2014**, *43*, 158–162. [CrossRef]